Development and evaluation of a dual-substrate model for a vapor-phase bioreactor
by Christopher Francis Wend

A thesis submitted in partial fulfillment of the requirements for the degree of Master of Science in Environmental Engineering
Montana State University

Abstract:
Christopher Francis Wend, 1994 To design, scale-up, and understand the processes of a vapor-phase bioreactor (VPBR), a phenomenologically-based mathematical model is developed to describe the VPBR. The numerical solution can then be used to evaluate bench-scale VP-BRs in preparation for pilot-scale VPBRs. To appropriately evaluate the model, the mass-transfer coefficients must be known for the operating conditions of the VPBR. To assess the mass-transfer coefficients within the VPBR, a non-reactive tracer was introduced into the VPBR and the mass-balance closed. From these studies, a corrected Onda correlation was developed. Use of the corrected Onda correlation allowed for the calculation and prediction of an enhancement factor for the liquid-side mass-transfer coefficient that was then used in the model. Model results were within 10 % of those from the bench-scale VPBRs.

DEVELOPMENT AND EVALUATION OF A DUAL-SUBSTRATE MODEL FOR A VAPOR-PHASE BIOREACTOR

by

Christopher Francis Wend

A thesis submitted in partial fulfillment
of the requirements for the degree

of

Master of Science

in

Environmental Engineering

MONTANA STATE UNIVERSITY
Bozeman, Montana

August 1994

APPROVAL

of a thesis submitted by

Christopher Francis Wend

This thesis has been read by each member of the thesis committee and has been found to be satisfactory regarding content, English usage, format, citations, bibliographic style and consistency and is ready for submission to the College of Graduate Studies.

August 11, 1994
Date

Chairperson, Graduate Committee

Approved for the Major Department

11 Aug '94
Date

Head, Major Department

Approved for the College of Graduate Studies

8/12/94
Date

Graduate Dean

STATEMENT OF PERMISSION TO USE

In presenting this thesis in partial fulfillment of the requirements for a master's degree at Montana State University, I agree that the Library shall make it available to borrowers under rules of the Library.

If I have indicated my intention to copyright this thesis by including a copyright notice page, copying is allowable only for scholarly purposes, consistent with "fair use" as prescribed in the U.S. Copyright Law. Requests for permission for extended quotation from or reproduction of this thesis in whole or in parts may be granted only by the copyright holder.

Signature 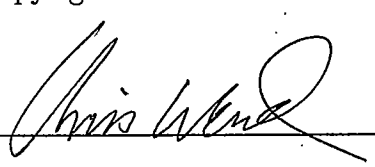

Date 8/11/94

ACKNOWLEDGEMENTS

The work presented in this thesis was funded by Orange County Water District, CA, and the National Water Research Institute. I wish to thank Dr. Warren Jones for giving me the opportunity to work on his project and to be his student. I wish to thank Dr. Stewart and Dr. Lewandowski for being excellent mentors. Finally, I wish to thank my wife, Tammy, and my children, Jeff, Alex, and Erica, for enduring academia with me.

TABLE OF CONTENTS

TABLE OF CONTENTS - Continued

TABLE OF CONTENTS - Continued

LIST OF TABLES

Table Page

LIST OF TABLES - Continued

Table Page

LIST OF FIGURES

Figure Page

ABSTRACT

DEVELOPMENT AND EVALUATION OF A DUAL-SUBSTRATE MODEL FOR A VAPOR-PHASE BIOREACTOR

Christopher Francis Wend, 1994

To design, scale-up, and understand the processes of a vapor-phase bioreactor (VPBR), a phenomenologically-based mathematical model is developed to describe the VPBR. The numerical solution can then be used to evaluate bench-scale VPBRs in preparation for pilot-scale VPBRs. To appropriately evaluate the model, the mass-transfer coefficients must be known for the operating conditions of the VPBR. To assess the mass-transfer coefficients within the VPBR, a non-reactive tracer was introduced into the VPBR and the mass-balance closed. From these studies, a corrected Onda correlation was developed. Use of the corrected Onda correlation allowed for the calculation and prediction of an enhancement factor for the liquid-side mass-transfer coefficient that was then used in the model. Model results were within 10 % of those from the bench-scale VPBRs.

CHAPTER 1

INTRODUCTION

Many industrial processes produce gas streams that are contaminated with volatile organic compounds (VOCs). In addition, remediation technologies such as soil vapor extraction (SVE), and air sparging of pumped groundwater, produce lean contaminated gas streams. These gas streams are being regulated more tightly with each version of the National Ambient Air Quality Standards (NAAQS) and it may come to the point where release of VOCs will be strictly prohibited.

A big problem currently faced across the nation is leaking underground storage tanks (LUST) that contain petroleum hydrocarbons such as gasoline and diesel fuel. As of February, 1993, there were 217,000 confirmed releases from underground storage tanks (USTs) awaiting cleanup, 75,000 confirmed cleanups, and 165,000 cleanups initiated, but not completed, in the United States (UST Workshop 1993) .

The treatment technologies available for remediating these sites include pump and treat and SVE. Remediation activity at approximately 7% of these sites will produce a contaminated vapor stream. In addition, the EPA is pushing alternative technologies, such as SVE, in the cleanup of LUSTs (UST Workshop 1993). This trend should increase the production of contaminated gas streams.

To treat a gas stream for volatile organic compounds (VOCs), traditional tech-

nologies employ either a phase change for the VOCs, or techniques such as thermal or catalytic oxidation in vapor incinerators. Vapor incinerators present high capital costs along with annual operation and maintenance costs needed for the process. In the case of a phase change, the VOC is not destroyed and must subsequently be disposed of in accordance with regulations. This method results in contaminated end products that will be increasingly more difficult to treat, or dispose of, due to tighter regulations.

To offer an alternative treatment technology, researchers have introduced biofilters and more recently vapor phase bioreactors (VPBR). A VPBR is a gas absorption column with an active biofilm attached to an inert artificial packing. The biofilm acts as a heterogeneous catalyst that mineralizes the VOCs in question. The activity of the biofilm is the key to the performance of the VPBR. Constant gas and liquid feeds are provided, and the VPBR may be operated in cocurrent or counter-current flow configurations. The liquid flow rate is kept small to minimize mass-transfer resistance, and recycle of liquid may be practiced, all but eliminating a liquid effluent stream.

Goals and Objectives

The main goal of this work was to develop a phenomenologically-based mathematical model to describe the steady-state operation of a VPBR. The numerical solution of the mathematical model could then be used to understand the processes within the VPBR and to aid in scale-up for pilot-scale VPBRs. Once the model was derived

from a conceptual model, there were a number of input parameters that needed to be determined within a reasonable amount of accuracy. The parameters that are incorporated in the model may be grouped into four general categories. These are

(1) physical constants (e.g. column dimensions, diffusivity, packing characteristics, and geometry)

(2) mass-transfer coefficients and Henry's Law constant

(3) biofilm physical constants (e.g. density, thickness, effect on diffusivity)

(4) biofilm kinetic constants.

The physical constants in (1) are well documented in literature such as *Perry's Chemical Engineering Handbook,* 6^{th} *ed.*, and the dimensions of the reactor and packing can be measured or supplied by the manufacturer. The biofilm constants in (3) and (4) have a range of values in the literature that can be used to estimate the values in the VPBR. For the mass transfer coefficients, it was determined that Onda correlations were the most robust in air stripping of VOCs (Lamarche and Droste 1989, Roberts, et al 1985), but had not been evaluated in biofilm reactor systems performing gas absorption. In addition, the effect of biofilm reaction on the liquid-side mass-transfer coefficients was unknown. To adequately predict the enhancement factor that would predict the true liquid-side mass-transfer coefficient with reaction present, knowledge of the pure physical mass-transfer coefficients was necessary.

Four objectives were set forth for obtaining the goal of developing a model to describe a VPBR. These were:

(1) Develop a phenomenologically-based mathematical model.

(2) Develop a computer model to solve the model in item (1).

(3) Evaluate model results against bench-scale data.

(4) Evaluate overall physical mass-transfer coefficients.

Experimental Approach

To determine the actual physical overall mass-transfer coefficients, three experiments were conducted to arrive at an observed pure physical overall mass-transfer coefficient for a VPBR with a biofilm present. These experiments are described below.

(1) The reactor organisms were plated on minimal media without an electron donor, and incubated in the presence of various VOCs that were similar to toluene in MW, solubility, and Henry's law constant. The VOC that produced no growth was then selected as the non-reactive tracer for the study.

(2) The Henry's Law constant for the nonreactive tracer chosen from the above item was then experimentally determined using reactor effluent.

(3) Tracer studies in the VPBR were then conducted to estimate an observed overall mass-transfer coefficient.

CHAPTER 2

BACKGROUND

Gas Absorption

Gas absorption is the process where one or more chemical species transfers from the gas phase across a gas-liquid interface and into the liquid phase. If there is no subsequent reaction in the liquid phase, then the absorption process is said to be pure physical absorption. Pure physical absorption into a quiescent liquid occurs through diffusion alone. If the liquid is agitated, then advection also plays a role in transferring the chemical species into the liquid. Most industrial and laboratory processes fall into this category. To model this process, several theories have been put forth. The easiest to visualize and use is the film model. The film model imagines a uniform stagnant film of thickness δ at the surface of the liquid in contact with the gas. The assumptions that there is a stagnant layer, and that it is uniformly thick, are both poor. However, predictions using this model are usually quite close to the predictions made by more sophisticated models such as the still surface and surface renewal models.

The film model leads to the following mathematical model.

$$R = \frac{\mathcal{D}_S(S^* - S^o)}{\delta} \tag{1}$$

$$k_L = \frac{\mathcal{D}_S}{\delta} \tag{2}$$

In equation (1), R is the average rate of transfer of gas per unit area, S^* is the concentration of dissolved gas corresponding to the partial pressure of the gas at the interface between the gas and liquid, S^o is the average concentration of the dissolved gas in the bulk of the liquid, and $\mathcal{D}_S$ is the diffusivity of the gas in the liquid. In equation (2), k_L is the physical mass-transfer coefficient for the liquid side. The film thickness, δ, accounts for the system hydrodynamic properties such as liquid flow, geometry, and other physical properties.

When there is gas absorption with a simultaneous chemical reaction in the liquid phase, then the overall rate of absorption can be greater than with physical gas absorption alone. To account for this enhanced absorption rate, researchers have introduced the concept of an enhancement factor, or reaction factor, defined as

$$E = \frac{k_L^*}{k_L} \geq 1. \tag{3}$$

Where k_L^* =mass-transfer coefficient with reaction and k_L =mass-transfer coefficient for pure physical absorption.

Two industrially important processes where gas absorption with reaction leads to an enhanced overall absorption rate are;

(1) absorption of hydrogen sulfide gas into solutions of amines.

(2) absorption of carbon dioxide into alkaline solutions of carbonates or amines.

In both of these situations, the kinetics of the reactions are simple, fairly well understood, and occur fast enough to proceed in the film layer next to the gas-liquid interface. In this case, the calculation of an enhancement factor for the liquid-side mass-transfer coefficient may be made (Danckwerts 1970). For first-order reaction kinetics and a fast reaction rate, it can be shown that the enhancement factor for k_L is

$$E = \frac{\sqrt{\mathcal{D}_S k_1}}{k_L} \tag{4}$$

where E is the enhancement factor for k_L, the physical mass-transfer coefficient, and k_1 is the first-order reaction-rate constant. As can be seen from (4), adequate knowledge of k_L is necessary for the estimation of E.

Gas absorption in a packed column is a standard way of increasing the gas-liquid interfacial contact area by forcing gas and liquid through an artificial, uniform, inert packing material. The packing may be dumped (random) packing, where uniform pieces of packing material are dumped into a vertical cylinder, or structured packing, where the packing is made into large pieces and fit into the column as large structural units. The gas and liquid phases are then forced through the column in either a cocurrent or counter-current configuration. In cocurrent configuration, the gas and liquid phases flow in the same direction (typically down) through the column. In counter-current configuration the gas flow is opposite to the flow of the liquid.

Mass-Transfer Correlations

To predict k_L and k_G (the mass transfer coefficient for gas-side mass transfer) for an application, it is necessary to include turbulent mixing, eddy mixing, diffusion, and other phenomena that influence the process of physical mass transfer. These phenomena are not easy to predict. Hence, mass transfer correlations have been developed to overcome these difficulties.

In the quest to find a method of determining physical mass-transfer coefficients, many correlations have been developed. Some of the more popular correlations include:

(1) Sherwood-Holloway (1940)

(2) Shulman (1955)

(3) Onda (1968)

These correlations are semi-empirical in nature. That is, they are empirically fit with bench-scale data, but the model that is fit usually includes dimensionless groups that describe the properties and/or the configuration of the system. For instance, these correlations take into account the viscosity, density, and velocities of the fluids and chemical species involved as well as the physical properties of the packing materials used in the columns. Other properties may be included, or excluded, according to how the particular researcher developed the correlation..

Onda correlations were chosen on the basis that they were robust with respect to a wide range of flow regimes and they were developed for random packings (e.g. Raschig rings). Studies by Roberts, et al, 1985, and Lamarche, et al, 1989, both show Onda to be a very robust correlation for air stripping. Onda also predicts individual local mass-transfer coefficients along with an effective gas-liquid interfacial area which are useful in other mass transfer calculations (e.g. enhancement factor).

Onda Correlations

Onda predicts the individual local mass-transfer coefficients for both the gas and liquid phases. An effective wetted surface area is predicted separately to assess the gas-liquid interface available for pure mass transfer to occur in the reactor. The correlations are given below.

$$k_L = 0.0051 \left(\frac{L_M}{a_w \mu_L}\right)^{\frac{2}{3}} \left(\frac{\mu_L}{\rho_L \mathcal{D}_L}\right)^{-\frac{1}{2}} (a_t d_p)^{0.4} \left(\frac{\rho_L}{\mu_L g}\right)^{-\frac{1}{3}} \tag{5}$$

$$k_G = 2 a_t \mathcal{D}_G \left(\frac{G_M}{a_t \mu_G}\right)^{0.7} \left(\frac{\mu_G}{\rho_G \mathcal{D}_G}\right)^{\frac{1}{3}} (a_t d_p)^{-2} \tag{6}$$

$$a_w = a_t[1 - exp[-1.45 \left(\frac{\sigma_c}{\sigma_L}\right)^{0.75} (Re_L)^{0.1} (Fr_L)^{-0.05} (We_L)^{0.2}]] \tag{7}$$

Where

a_w = Wetted specific surface area $[=] \frac{area}{volume}$

a_t = Total specific surface area $[=] \frac{area}{volume}$

L_M = Liquid mass flux $[=] \frac{mass}{area\ time}$

G_M = Gas mass flux [=] $\frac{mass}{area\ time}$

μ_L = Viscosity of liquid [=] $\frac{mass}{length\ time}$

μ_G = Viscosity of gas [=] $\frac{mass}{length\ time}$

ρ_L = Density of liquid [=] $\frac{mass}{volume}$

ρ_G = Density of gas [=] $\frac{mass}{volume}$

$\mathcal{D}_L$ = Liquid diffusion coefficient [=] $\frac{length^2}{time}$

$\mathcal{D}_G$ = Gas diffusion coefficient [=] $\frac{length^2}{time}$

d_p = Average size of packing [=] $length$

g = Gravitational Constant [=] $\frac{length}{time^2}$

σ_c = Surface tension of packing material [=] $\frac{force}{length}$

σ_L = Surface tension of liquid [=] $\frac{force}{length}$

$Re_L = \frac{L_M}{a_t \mu_L}$ = Liquid-phase Reynolds number (dimensionless)

$Fr_L = \frac{{L_M}^2 a_t}{{\rho_L}^2 g}$ = Liquid-phase Froude number (dimensionless)

$We_L = \frac{{L_M}^2}{\rho_L \sigma_L a_t}$ = Liquid-phase Weber number (dimensionless)

In the model development in Chapter 3, two-resistance theory is employed to account for the overall mass transfer resistance between the gas and liquid phases. In addition, the use of overall mass-transfer coefficients is employed to simplify the calculations.

This approach is standard (Sherwood 1937, Treybal 1980, Sherwood 1975) when the gas is lean and volatile. The overall mass-transfer coefficients are calculated using the following equations.

$$\frac{1}{K_G} = \frac{1}{k_G} + \frac{K_H \mathcal{V}_g}{\mathcal{V}_l k_L} \tag{8}$$

$$\frac{1}{K_L} = \frac{\mathcal{V}_l}{K_H \mathcal{V}_g k_G} + \frac{1}{k_L} \tag{9}$$

Where K_H is Henry's Law constant, $\mathcal{V}_g$ is the molar volume of the gas phase, and $\mathcal{V}_l$ is the molar volume of the liquid phase.

Since the VOCs in this study were quite volatile, the liquid side is the controlling phase. The overall liquid-side mass-transfer coefficient (k_L) is then independent of gas flow rate (Roberts, et al, 1985). In addition, Onda is within 30% of predicting k_G (Thom and Byers, 1993). Using the overall mass-transfer data, k_L for the tracer study may be calculated.

Biofilm Correlations

Wilson and Geankoplis, 1966, proposed a correlation for mass transfer between water and solid spheres at low Reynolds numbers . This correlation is shown in equation (10).

$$k_{L_B} = 1.09 L_M \left(\frac{\mu_L}{\rho_L D_L}\right)^{-\frac{2}{3}} \left(\frac{d_p L_M}{\mu_L}\right)^{-\frac{2}{3}} \tag{10}$$

The input parameters are the same as described before, and k_{L_B} is the mass transfer coefficient from bulk liquid to biofilm $\left(\frac{length}{time}\right)$.

Biofilms

The study of biofilms is a relatively new subject in the scientific community. The first study occurred in 1943 and further research was slow until the early 1970s (Characklis and Marshall, 1990). Research of biofilms represents a new way of studying bacteria in that the bacteria are studied in their natural state, biofilms, instead of planktonic batch cultures.

Biofilms are created by bacteria when they attach to a surface. The bacteria secrete an extracellular polymer that surrounds the cells and enables the cells to attach to each other and to surfaces. It is thought that the biofilm mode of growth serves many purposes such as protection against dehydration and predators. Biofilms also provide resistance to diffusion of chemical species. This is an advantage when the chemical species may harm the organisms. Thicknesses vary from less than one layer of cells (monolayer) to $>300mm$ in microbial mats.

The entire structure of the biofilm is quite porous and is generally >95% water. Biofilms are characterized by structural, chemical, and ecological heterogeneity. In addition, there are usually large amounts of particulates and larger organisms in a biofilm.

Since the bacteria in a biofilm are actively reproducing and respiring, there is a reaction rate associated with the substances that the bacteria are consuming. Biofilm kinetics are usually described with expressions like Monod or Haldane kinetics. Monod kinetics are the most widely used biofilm kinetic expression, and represents a mixture

of zero and first-order kinetics.

$$\mu(S) = \mu_m \left(\frac{S}{K_s + S}\right) \tag{11}$$

Where

S = limiting substrate concentration [=] $\frac{kg}{m^3}$

μ_{max} = maximum specific cell growth rate [=] $\frac{1}{day}$

K_s = limiting substrate half-saturation coefficient [=] $\frac{kg}{m^3}$

Dual Monod kinetics are used in this study to account for the depletion of two substrates by the biofilm (12).

$$\mu(S,O) = \mu_m \left(\frac{S}{K_s + S}\right)\left(\frac{O}{K_o + O}\right). \tag{12}$$

Where

S = electron-donor concentration [=] $\frac{kg}{m^3}$

O = electron-acceptor concentration [=] $\frac{kg}{m^3}$

μ_{max} = maximum specific cell growth rate [=] $\frac{1}{day}$

K_s = electron-donor half-saturation coefficient [=] $\frac{kg}{m^3}$

K_o = electron-acceptor half-saturation coefficient [=] $\frac{kg}{m^3}$

The kinetic constants are usually determined using batch or chemostat techniques. These techniques are well documented in the literature (Characklis and Marshall, 1990).

Biofilm Modeling

Biofilm behavior is a cumulative response to biological, chemical, and physical factors in the environment. To understand these processes more thoroughly, and to aid in the study of the factors responsible for a biofilm's response, phenomenologically-based mathematical models are often developed. These models are useful in determining which factors control the behavior of the biofilm.

Often, knowledge of the fate of certain chemicals within the biofilm is wanted. Thus, models have been produced that describe the utilization of chemical species within a biofilm.

There have been many models proposed to model the diffusion and reaction of chemical species within a biofilm (e.g. Rittman and McCarty 1981, Skowlund 1990). Most biofilm modeling has been done with biofilm-liquid phases only. These models seek to incorporate physical properties such as diffusion, reaction, biofilm density, and biofilm reaction rate as some of the quantifiable properties in a biofilm. One-dimensional models have done quite well in describing substrate and electron-acceptor depletion within biofilms.

Biofilters

A form of bioreactor that has been extensively used in the treatment of gas streams that produce odor and, more recently, that contain VOCs, is the biofilter. A biofilter

usually consists of several compartments filled with organic soils and materials which support a biofilm and provide an adsorptive surface. The problem with these types of reactors is that they can take up a large amount of space and they do not have a very quantifiable surface area or adsorptive characteristics. Researchers have been able to model biofilters using a gas/biofilm model (Baltzis, 1993).

The accurate knowledge of an artificial, inert, substratum's physical characteristics, and the presence of a liquid phase, are the attractive features of a VPBR.

Vapor-phase Bioreactors

Vapor-phase Bioreactors (VPBRs) are a blend of traditional gas absorption in a packed column with the reaction from a biofilm. The organisms chosen for a VPBR biofilm are environmental isolates, or consortia, that have the ability to degrade the volatile organic compound(s) that will be applied to the column.

Use of a manufactured packing allows for a more complete assessment of the surface area and flow characteristics inside the VPBR. There are a large number of correlations for mass transfer coefficients in gas absorbers using manufactured packing. Since the VPBR is a gas absorber, knowledge of the mass transfer coefficients within the VPBR is essential for modeling and scale-up.

In VPBRs, the liquid flow rates are quite low compared to traditional gas absorber liquid flow rates. The presence of a biofilm reduces the amount of channeling and increases the wetted surface area. This sponge effect also increases the thickness of

the liquid-biofilm phase.

VPBRs are also known as biological trickling filters by Diks, 1992, and bioscrubbers by Overcamp, et al, 1991. Both Overcamp,et al, and Diks employed liquid recirculation as an operating configuration. This led to an assumption that there was a constant concentration of the chemical species in the liquid phase.

CHAPTER 3

MODEL DEVELOPMENT

The development of a mathematical model for a physical system began with a conceptual model of the processes involved. The three phases present in a VPBR are the biofilm, liquid, and gas phases. Figure 1 shows a microscale conceptual model of the three phases in a flat plate geometry configuration.

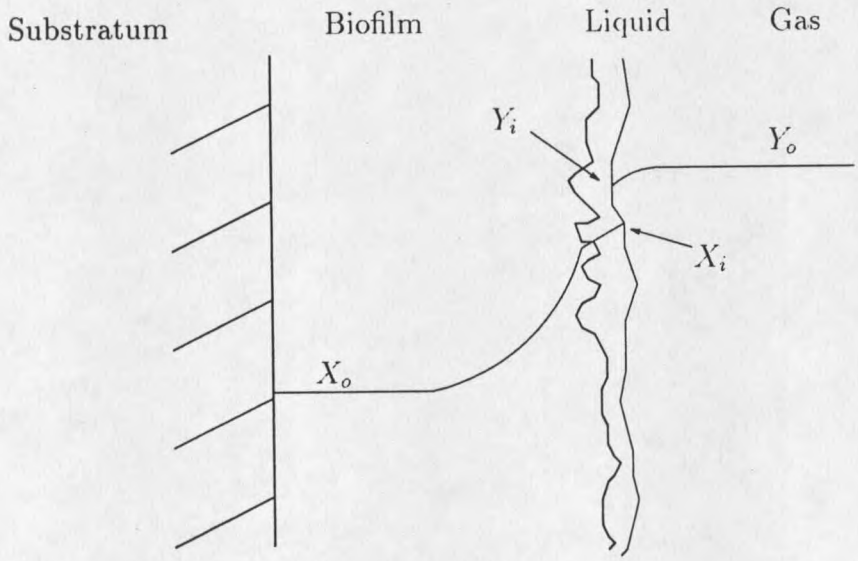

Figure 1: Microscale Conceptual Model.

The flux at the interface of the biofilm is then used to determine the amount of removal of contaminant from a differential macroscale slice in a VPBR. Figure 2 shows a macroscale conceptual model of a VPBR.

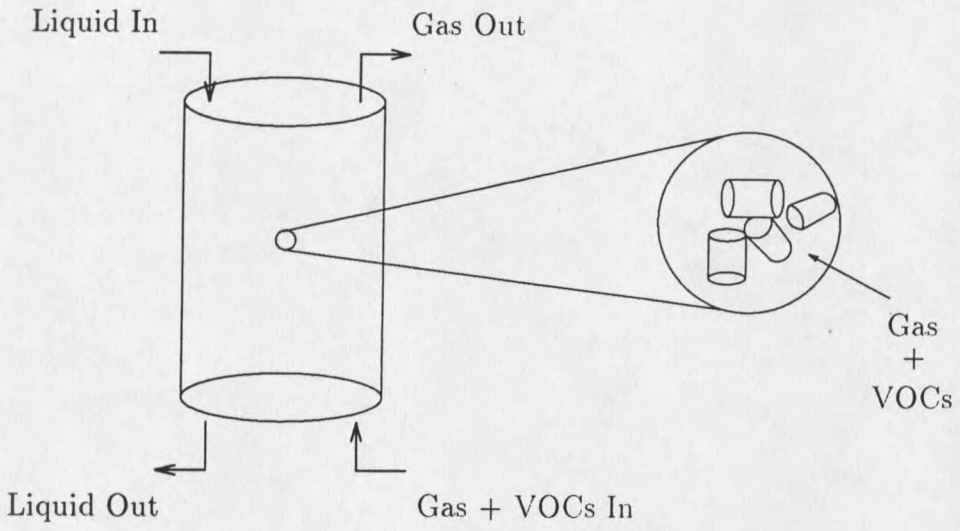

Figure 2: Macroscale Conceptual Model.

Microscale Model Equations

Development of the microscale model equations begins by looking at a control volume as shown in Figure 3.

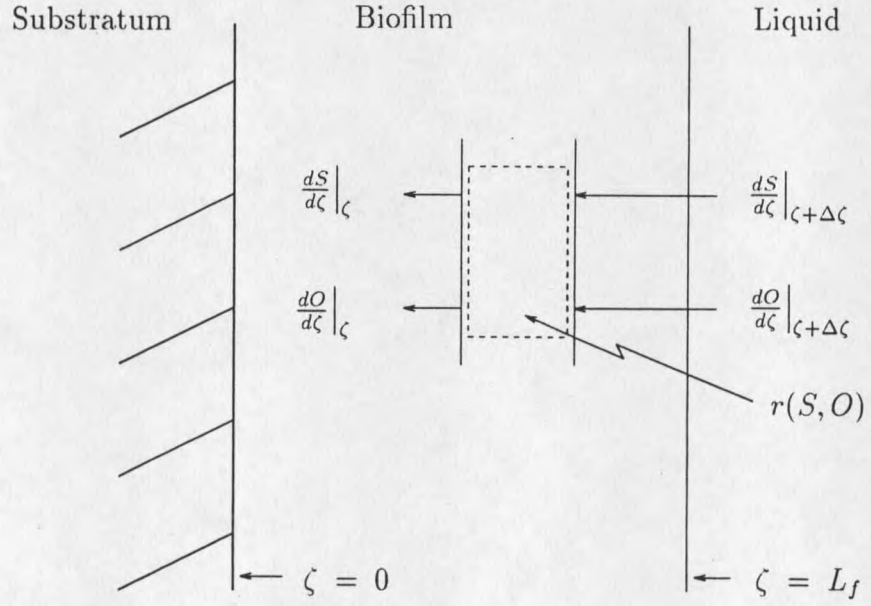

Figure 3: Microscale Mass Balance.

In the biofilm, it is assumed that dual Monod kinetics describe the reaction rate with the electron-donor and the electron-acceptor. Dual Monod kinetics may be described as,

$$\mu(S,O) = \mu_m \left(\frac{S}{K_s+S}\right)\left(\frac{O}{K_o+O}\right). \tag{13}$$

where the reaction rates are

$$r_s = \frac{\mu(S,O)\rho_f}{Y_{x/d}} \tag{14}$$

and

$$r_o = \frac{\mu(S,O)\rho_f}{Y_{x/a}} \tag{15}$$

where ρ_f is the biofilm concentration, $Y_{x/d}$ is the yield of biomass from substrate (electron-donor), and $Y_{x/a}$ is the yield of biomass from oxygen (electron-acceptor). Taking a mass balance of the electron-donor, electron-acceptor, and a single species of bacteria over the control volume shown in Figure 3, and assuming Fick's law holds, yields,

$$\mathcal{D}_d \left.\frac{dS}{d\zeta}\right|_{\zeta+\Delta\zeta} = \mathcal{D}_d \left.\frac{dS}{d\zeta}\right|_{\zeta} + \frac{\mu_m \rho_f}{Y_{x/d}}\left(\frac{S}{K_s+S}\right)\left(\frac{O}{K_o+O}\right)\Delta\zeta. \tag{16}$$

$$\mathcal{D}_a \left.\frac{dO}{d\zeta}\right|_{\zeta+\Delta\zeta} = \mathcal{D}_a \left.\frac{dO}{d\zeta}\right|_{\zeta} + \frac{\mu_m \rho_f}{Y_{x/a}}\left(\frac{S}{K_s+S}\right)\left(\frac{O}{K_o+O}\right)\Delta\zeta. \tag{17}$$

Assuming $\mathcal{D}_d$ and $\mathcal{D}_a$ are constant and taking limits

$$\mathcal{D}_d \lim_{\Delta\zeta\to 0}\left(\frac{\left.\frac{dS}{d\zeta}\right|_{\zeta+\Delta\zeta} - \left.\frac{dS}{d\zeta}\right|_{\zeta}}{\Delta\zeta}\right) = \lim_{\Delta\zeta\to 0}\frac{\mu_m\rho_f}{Y_{x/d}}\left(\frac{S}{K_s+S}\right)\left(\frac{O}{K_o+O}\right). \tag{18}$$

$$\mathcal{D}_a \lim_{\Delta\zeta \to 0} \left(\frac{\frac{dO}{d\zeta}\Big|_{\zeta+\Delta\zeta} - \frac{dO}{d\zeta}\Big|_{\zeta}}{\Delta\zeta} \right) = \lim_{\Delta\zeta \to 0} \frac{\mu_m \rho_f}{Y_{x/a}} \left(\frac{S}{K_s + S} \right) \left(\frac{O}{K_o + O} \right). \tag{19}$$

yields the following 2^{nd}-order, non-linear, non-homogeneous, coupled system of ordinary differential equations.

$$\mathcal{D}_d \frac{d^2 S}{d\zeta^2} = \frac{\mu_m \rho_f}{Y_{x/d}} \left(\frac{S}{K_s + S} \right) \left(\frac{O}{K_o + O} \right) \tag{20}$$

$$\mathcal{D}_a \frac{d^2 O}{d\zeta^2} = \frac{\mu_m \rho_f}{Y_{x/a}} \left(\frac{S}{K_s + S} \right) \left(\frac{O}{K_o + O} \right) \tag{21}$$

With the following boundary conditions.

$$\frac{dS}{d\zeta}(0) = 0 \tag{22}$$

$$\mathcal{D}_d \frac{dS}{d\zeta}(L_f) = K_{L_B d} \left(S_{bulk} - S_{L_f} \right) \tag{23}$$

$$\frac{dO}{d\zeta}(0) = 0 \tag{24}$$

$$\mathcal{D}_a \frac{dO}{d\zeta}(L_f) = K_{L_B a} \left(O_{bulk} - O_{L_f} \right) \tag{25}$$

Where

S = electron-donor concentration $[=] \frac{kg}{m^3}$

O = electron-acceptor concentration $[=] \frac{kg}{m^3}$

ζ = spatial dimension in biofilm $[=] m$

L_f = biofilm thickness $[=] m$

$\mathcal{D}_d$ = electron-donor diffusivity in biofilm [=] $\frac{m^2}{day}$

$\mathcal{D}_a$ = electron-acceptor diffusivity in biofilm [=] $\frac{m^2}{day}$

μ_{max} = maximum specific cell growth rate [=] $\frac{1}{day}$

ρ_f = biofilm density [=] $\frac{kg}{m^3}$

$Y_{x/d}$ = yield of cells/electron donor [=] $\frac{kg\ biomass}{kg\ donor}$

$Y_{x/a}$ = yield of cells/electron acceptor [=] $\frac{kg\ biomass}{kg\ acceptor}$

K_{L_Bd} = electron-donor mass-transfer coefficient [=] $\frac{m}{day}$

K_{L_Ba} = electron-acceptor mass-transfer coefficient [=] $\frac{m}{day}$

K_d = electron-donor half-saturation coefficient [=] $\frac{kg}{m^3}$

K_a = electron-acceptor half-saturation coefficient [=] $\frac{kg}{m^3}$

Boundary conditions (22) and (24) represent zero flux conditions at the substratum while (23) and (25) are matching flux conditions at the biofilm-liquid interface.

Introducing the dimensionless variables, $K_{sd} = \frac{K_s}{S_{bulk}}$, $K_{sa} = \frac{K_o}{O_{bulk}}$, $X_d = \frac{S}{S_{bulk}}$, $X_a = \frac{O}{O_{bulk}}$, and $\delta = \frac{\zeta}{L_f}$, yields the following dimensionless form of the microscale equations.

$$\frac{d^2X_d}{d\delta^2} = \frac{\mu_m \rho_f L_f^2}{Y_{x/d}\mathcal{D}_d}\left(\frac{X_d}{K_{sd}+X_d}\right)\left(\frac{X_a}{K_{sa}+X_a}\right) \tag{26}$$

$$\frac{d^2X_a}{d\delta^2} = \frac{\mu_m \rho_f L_f^2}{Y_{x/a}\mathcal{D}_a}\left(\frac{X_d}{K_{sd}+X_d}\right)\left(\frac{X_a}{K_{sa}+X_a}\right) \tag{27}$$

With the following boundary conditions.

$$\frac{dX_d}{d\delta}(0) = 0 \tag{28}$$

$$\frac{dX_d}{d\delta}(1) = \frac{K_{L_B d} L_f}{\mathcal{D}_d}\left(1 - X_{d_{L_f}}\right) \tag{29}$$

$$\frac{dX_a}{d\delta}(0) = 0 \tag{30}$$

$$\frac{dX_a}{d\delta}(1) = \frac{K_{L_B a} L_f}{\mathcal{D}_a}\left(1 - X_{a_{L_f}}\right) \tag{31}$$

For a discussion of the solution method, see Appendix A.

Macroscale Model Equations

The solution of the microscale model equations gives the flux of the electron-donor and electron-acceptor into the biofilm as a function of liquid concentrations of the electron-donor and electron-acceptor. This information can be used with an effective surface area to scale up the flux to a macroscale flux in a differential slice taken through the VPBR.

Counter-Current Flow

Figure (4) shows a conceptualization of the macroscale mass balance over the VPBR configured for counter-current flow configuration. The mass balance yields

$$y_d(t + \Delta t) = y_d(t) - \frac{K_{Gd} a K_{Hd}}{v_g}\left(\frac{y_d}{K_{Hd}} - x_d\right)\Delta t \tag{32}$$

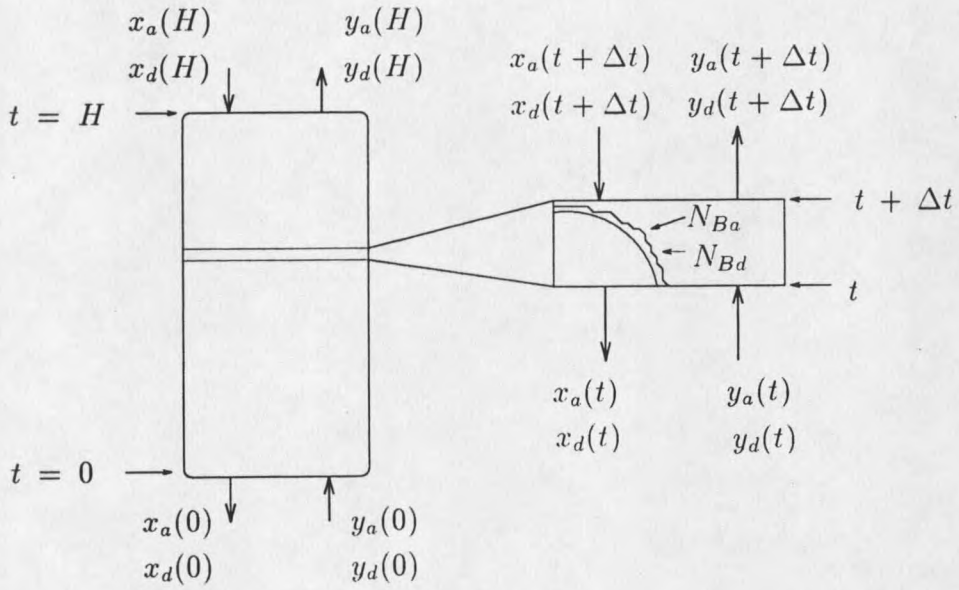

Figure 4: Macroscale Mass Balance (Counter-Current Flow).

$$x_d(t + \Delta t) + \frac{K_{Ld}a}{v_l}\left(\frac{y_d}{K_{Hd}} - x_d\right)\Delta t - \frac{N_{Bd}a_f\mathcal{V}_l}{v_l}\Delta t = x_d(t) \tag{33}$$

$$y_a(t + \Delta t) = y_a(t) - \frac{K_{Ga}aK_{Ha}}{v_g}\left(\frac{y_a}{K_{Ha}} - x_a\right)\Delta t \tag{34}$$

$$x_a(t + \Delta t) + \frac{K_{La}a}{v_l}\left(\frac{y_a}{K_{Ha}} - x_a\right)\Delta t - \frac{N_{Ba}a_f\mathcal{V}_l}{v_l}\Delta t = x_a(t) \tag{35}$$

Dividing by Δt and taking the limits as $\Delta t \to 0$ yields the macroscale model equations.

$$\frac{dy_d}{dt} = \frac{K_{Gd}aK_{Hd}}{v_g}\left(x_d - \frac{y_d}{K_{Hd}}\right) \tag{36}$$

$$\frac{dx_d}{dt} = \frac{K_{Ld}a}{v_l}\left(x_d - \frac{y_d}{K_{Hd}}\right) + \frac{N_{Bd}a_f\mathcal{V}_l}{v_l} \tag{37}$$

$$\frac{dy_a}{dt} = \frac{K_{Ga}aK_{Ha}}{v_g}\left(x_a - \frac{y_a}{K_{Ha}}\right) \tag{38}$$

$$\frac{dx_a}{dt} = \frac{K_{La}a}{v_l}\left(x_a - \frac{y_a}{K_{Ha}}\right) + \frac{N_{Ba}a_f\mathcal{V}_l}{v_l} \tag{39}$$

Where,

$$N_{Bd} = \mathcal{D}_d \frac{dx_d}{d\delta}(L_f) \tag{40}$$

and

$$N_{Ba} = \mathcal{D}_a \frac{dx_a}{d\delta}(L_f). \tag{41}$$

The boundary conditions for counter-current flow are given below.

$$y_d(0) = y_{do} \tag{42}$$

$$x_d(H) = 0 \tag{43}$$

$$y_a(0) = y_{ao} \tag{44}$$

$$x_a(H) = 0 \tag{45}$$

Introducing the dimensionless variables, $Y_d = \frac{y_d}{y_{do}}$, $X_d = \frac{x_d K_{Hd}}{y_{do}}$, $Y_a = \frac{y_a}{y_{ao}}$, $X_a = \frac{x_a K_{Ha}}{y_{ao}}$, and $z = \frac{t}{H}$, yields the following dimensionless form of the macroscale equations.

$$\frac{dY_d}{dz} = \alpha_{1d}(X_d - Y_d) \tag{46}$$

$$\frac{dX_d}{dz} = \alpha_{2d}(X_d - Y_d) + \alpha_{3d}N_{Bd} \tag{47}$$

$$\frac{dY_a}{dz} = \alpha_{1a}(X_a - Y_a) \tag{48}$$

$$\frac{dX_a}{dz} = \alpha_{2a}(X_a - Y_a) + \alpha_{3a}N_{Ba} \tag{49}$$

Where,

$$N_{Bd} = \mathcal{D}_d \frac{dX_d}{d\delta}(L_f) \tag{50}$$

and

$$N_{Ba} = \mathcal{D}_a \frac{dX_a}{d\delta}(L_f). \tag{51}$$

The boundary conditions are given below.

$$Y_d(0) = 1 \tag{52}$$

$$X_d(1) = 0 \tag{53}$$

$$Y_a(0) = 1 \tag{54}$$

$$X_a(1) = 0 \tag{55}$$

In the analysis of this coupled, non-linear, non-homogeneous, system of ordinary differential equations it is sometimes convenient to express the equations in vector-matrix formulation. This formulation is shown below.

$$\frac{d}{dz}(\vec{x}) = A\vec{x} + \vec{y} \tag{56}$$